LAND DEGRADATION & DEVELOPMENT
Land Degrad. Develop. (2014)
Published online in Wiley Online Library (wileyonlinelibrary.com) **DOI**: 10.1002/ldr.2335

EVALUATING *IN SITU* WATER AND SOIL CONSERVATION PRACTICES WITH A FULLY COUPLED, SURFACE/SUBSURFACE PROCESS-BASED HYDROLOGICAL MODEL IN TIGRAY, ETHIOPIA

Emmanuel Opolot[1,2]*, Tesfay Araya[3], Jan Nyssen[4], Bashar Al-Barri[1], Koen Verbist[1,5], Wim M. Cornelis[1]

[1]*Department of Soil Management, Ghent University, Coupure Links 653, B-9000 Gent, Belgium*
[2]*Department of Geology and Soil Science, Ghent University, Krijgslaan 281 (S8), B-9000 Gent, Belgium*
[3]*Department of Dry Land Crop and Horticultural Science, Mekelle University, PO Box 231, Mekelle, Ethiopia*
[4]*Department of Geography, Ghent University, Krijgslaan 281 (S8), B-9000 Gent, Belgium*
[5]*UNESCO, Santiago, Chile*

Received: 28 October 2013; Revised: 20 July 2014; Accepted: 2 October 2014

ABSTRACT

In situ water and soil conservation (WSC) practices are a promising intervention to improve rainwater management particularly in the semi-arid to dry sub-humid tropics. This study applies a fully coupled surface–subsurface process-based model (HydroGeoSphere) to simulate in detail rainwater partitioning as affected by two *in situ* WSC practices [*terwah*+ (TER+) and *derdero*+ (DER+)] currently under study on Vertisols in Tigray, Ethiopia and to evaluate the treatments in terms of rainwater partitioning. In the TER+ practice, contour furrows of 0·2 m wide and 0·1 m deep are created at 1·5 m intervals between permanent broad beds, whereas in DER+, permanent raised beds 0·6 m wide with furrows 0·2 m wide and 0·1 m deep are created, to minimize runoff and water logging. The model accurately reproduced measured surface runoff (e.g. in DER+: Nash–Sutcliffe model efficiency $E = 0{\cdot}6$ for calibration and 0·7 for verification) and soil moisture content (DER+: $E = 0{\cdot}6$ for calibration and 0·8 for verification). Runoff depth was lowest under DER+ (50 mm) followed by TER+ (67 mm) and significantly higher in conventional tillage (CT) (160 mm). Simulated transpiration, evaporation and drainage out of the root zone were all higher under DER+ and TER+ compared with CT. The effects of DER+ and TER+ practices on rainwater partitioning were more pronounced in wet years than in dry years. The model proved to be a promising and versatile tool to assess the impact of WSC practices on rainwater partitioning at the field scale. Copyright © 2014 John Wiley & Sons, Ltd.

KEY WORDS: surface-subsurface flow model; water and soil conservation; Ethiopia

INTRODUCTION

Frequent droughts and floods continue to constrain the potential of rain-fed agriculture, yet this remains a major source of livelihood especially in sub-Saharan Africa. In addition, high runoff losses and unproductive evaporation have been cited as major causes of low yields in semi-arid areas (Rockström & Falkenmark, 2000). *In situ* water and soil conservation (WSC) practices are one of the viable strategies to improve rain-fed agriculture as they increase vegetative cover, improve soil properties and reduce runoff (FAO, 2002). According to Wallace (2000), principles of runoff reducing techniques are well-known, but there is still a need to investigate their effects on runoff processes for efficient and appropriate application of effective measures in the correct circumstances. Evaluation of *in situ* WSC has been mainly treated empirically (e.g. Makurira *et al*., 2007; Tesfay Araya *et al*., 2011, 2012, 2014a, 2014b), and only few studies (e.g. Boers, 1994; Verbist *et al*., 2009; 2012) have used a modelling approach to evaluate the efficiency of water-harvesting techniques. Although empirical studies give valuable insight to the onsite effects of WSC, they remain costly and time consuming. In addition, results from field experiments cannot be generalized and applied to other climatic and landscape environments (Verbist *et al*., 2012).

Continued advances in hydrological models provide an excellent opportunity to assist in continuous monitoring and evaluation of the effects of *in situ* WSC practices in different climatic and landscape environments. According to Soltani & Hoogenboom (2007), simulation models once validated provide cheaper and faster ways to test the efficiency of different WSC practices with limited data. However, as mentioned by Verbist *et al*. (2012), most modelling studies have used empirical models in which surface runoff is simply calculated as infiltration excess water and thus unable to describe all complex processes that influence surface runoff. Studies that have used physically based models to evaluate the efficiency of water-harvesting techniques (Boers, 1994; Verbist *et al*., 2009) have used models in which overland and subsurface flow are treated separately, thus unable to simultaneously describe complex processes of runoff and infiltration. To our knowledge, the only study in which the effects of WSC practices have been investigated with a fully coupled surface–subsurface model that allows the interaction of soil hydrological surface–subsurface

* Correspondence to: E. Opolot, Department of Soil Management, Ghent University, Coupure Links 653, B-9000 Gent, Belgium.
E-mail: Emmanuel.Opolot@ugent.be

processes was recently published by Verbist *et al.* (2012). The advantage of such models is that they allow detailed insight in the partitioning of rainwater as affected by *in situ* WSC practices and provide a versatile tool for improving their design. Until now, fully coupled surface–subsurface models have generally been applied at the larger scale of small to large catchments (e.g. Jones *et al.*, 2008; Sciuto & Diekkrüger, 2010; Qin *et al.*, 2013).

The purpose of this study is to apply a fully coupled surface–subsurface physically based model [HydroGeoSphere (HGS)] (1) to simulate in detail rainwater partitioning as affected by *in situ* WSC practices and (2) to evaluate two *in situ* WSC practices currently under study in Tigray, Ethiopia, in terms of rainwater partitioning for crop production.

MATERIALS AND METHODS

Study Site Description

The study area is Adigudem located at 13°14′N and 39°32′E, approximately 740 km from Addis Ababa at an altitude of 1,960 m.asl, in Tigray, northern Ethiopia (Figure 1). The climate in Adigudem is described as cool tropical semi-arid with recurrent droughts. The area receives mean annual rainfall of 512 mm, with more than 85% falling during the cropping season from mid-June to mid-September. The mean, minimum and maximum annual temperatures of Adigudem are 19, 11 and 27 °C, respectively, and mean annual potential evapotranspiration is 1,486 mm (Tesfay Araya *et al.*, 2011).

The soil in the study area has been classified as Pelli Calcic Vertisol according to World Reference Base for soil resources (WRB, 2006). Vertisols have very low infiltration rate and are thus susceptible to erosion as well as water logging. Efficient and well-tested *in situ* WSC practices are therefore necessary for sustainable productivity of these soils.

HydroGeoSphere Model

HydroGeoSphere is a three-dimensional model developed to simulate surface–subsurface water flow and solute transport at a larger watershed scale. The model uses a modified form of Richards' equation 1 to describe three-dimensional flow processes in the variably saturated subsurface:

$$-\nabla.(\omega_m q) + \sum\Gamma_{ex} \pm Q = \omega_m \frac{\partial}{\partial t}(\theta_s S_w) \tag{1}$$

Where: ω_m is the fraction of the total porosity occupied by the porous medium [dimensionless]. This term is equal to 1 as long as only one porous continuum is considered for a simulation, and q [L T^{-1}] is given by Equation 2:

$$q = -K_{\text{sat}}\, k_r\, (\psi)\nabla(\psi + Z) \tag{2}$$

Where: K_{sat} is the saturated hydraulic conductivity tensor [L T^{-1}], k_r represents the relative permeability of the medium with respect to S_w (degree of water saturation), ψ is the pressure head [L] and Z is the elevation head [L]. In Equation 1, θ_s is the saturated moisture content [dimensionless] and usually assumed to be equal to the porosity. Γ_{ex} [L^3 L^{-3} T^{-1}] is the volumetric fluid exchange rate,

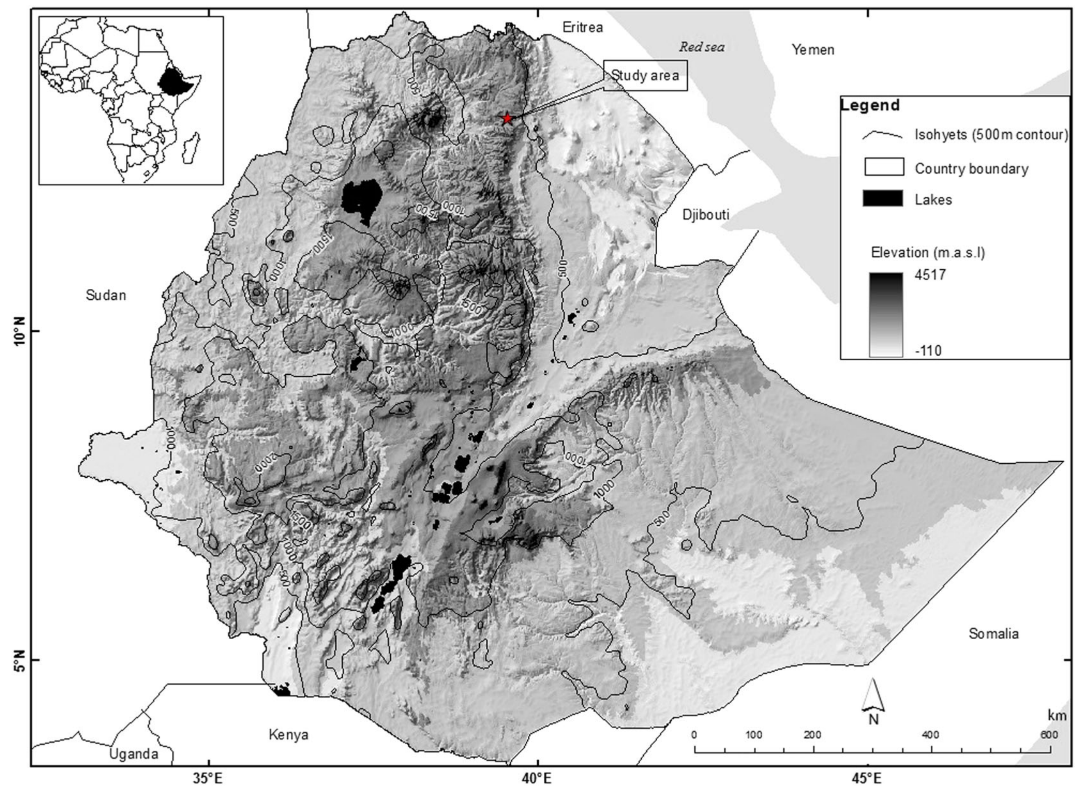

Figure 1. Map of Ethiopia showing the location of Adigudem (Source: Tesfay Araya *et al.*, 2012). This figure is available in colour online at wileyonlinelibrary.com/journal/ldr.

Q [$L^3 L^{-3} T^{-1}$] represents the fluid exchange with the outside of the simulation domain, specified from boundary conditions, and it is a volumetric fluid flux per unit volume representing a source or a sink to the porous medium system (Therrien *et al.*, 2010).

The HGS model applies two-dimensional Saint Venant equation 3 to describe surface flow:

$$\frac{\partial \phi_o h_o}{\partial t} - \frac{\partial}{\partial x}\left(d_o K_{ox}\frac{\partial h_o}{\partial x}\right) - \frac{\partial}{\partial y}\left(d_o K_{oy}\frac{\partial h_o}{\partial y}\right) + d_o \Gamma_o \pm Q_o = 0 \quad (3)$$

Where: d_o is the depth of flow [L], h_o represents the water surface elevation [L], Γ_o is the volumetric exchange rate [$L^3 L^{-3} T^{-1}$] between the surface flow and the subsurface flow, Q_o is a volumetric flow rate per unit area representing external sinks and sources [$L T^{-1}$], and ϕ_o is a surface flow domain porosity. K_{ox} and K_{oy} are surface conductance [$L T^{-1}$] in x and y directions, respectively. These variables depend on the equation used to approximate the friction slopes (Therrien *et al.*, 2010).

Surface–subsurface coupling in this study was by means of the Darcy flux relation to transfer water from one layer to another. The exchange flux between the surface and subsurface layers is given by the relation equation 4:

$$d_o \Gamma_o = \frac{k_r K_{zz}}{l_{exch}}(h - h_o) \quad (4)$$

Where: d_o as defined earlier is the flow depth, Γ_o is the exchange flux between surface and subsurface in which case a positive Γ_o represents an upward flow to the surface and a negative Γ_o implies otherwise, h_o and h represent the surface and subsurface water heads respectively, k_r is the relative permeability for the exchange flux, K_{zz} is the vertical saturated hydraulic conductivity of the underlying layer and l_{exch} is the coupling length that relates to the thickness of the assumed interface layer (Therrien *et al.*, 2010).

Interception and evapotranspiration processes are simulated in HGS on the basis of equations developed by Kristensen & Jensen (1975) and Wigmosta *et al.* (1994). The bucket type model is used to simulate interception process whereby only precipitation in excess of interception storage and evaporation reaches the ground surface. The amount of water stored by the interception process varies between zero and a maximum (S_{int}^{Max}), the interception storage capacity expressed in [L]. According to Kristensen & Jensen (1975), this factor depends on the vegetation type and the stage of development and is calculated using Equation 5:

$$S_{int}^{Max} = C_{int} LAI \quad (5)$$

Where: C_{int} is the empirical canopy storage parameter [L] and *LAI* is the dimensionless leaf area index. Rainfall and evaporation respectively are the processes that fill and deplete interception storage.

Evapotranspiration is simulated as a combination of plant transpiration and evaporation processes that affect both surface and subsurface flow domains. Transpiration (T_p) is influenced by the vegetation, soil moisture content and the root distribution function. It occurs within the root zone of the subsurface and is calculated using Equation 6 (Kristensen & Jensen, 1975):

$$T_p = f_1(LAI) f_2(\theta) RDF \left(E_p - E_{CAN}\right) \quad (6)$$

Where: f_1 (*LAI*) is a function of *LAI* [−], $f_2(\theta)$ is a function of nodal moisture content [−], *RDF* is the time-varying root distribution function [−], E_p is the potential evapotranspiration [$L T^{-1}$] and E_{CAN} is the evaporation of the intercepted water by the canopy [$L T^{-1}$]. The vegetation parameter, f_1 (*LAI*), is given in Equation 7 as follows:

$$f_1(LAI) = \max\{0, \min[1, (C_2 + C_1 LAI)]\} \quad (7)$$

Where: C_1 and C_2 are empirical constants, with respective standard values of 0·5 and 0.

The root density function, *RDF*, is defined as in Equation 8:

$$RDF = \frac{\int_{z_1'}^{z_2'} r_F(z')\,dz'}{\int_0^{L_r} r_F(z')\,dz'} \quad (8)$$

Where: L_r is the effective root length [L], z' is the depth from the soil surface [L] and r_F (z') is the logarithmic root extraction function. The RDF can have a constant, linear, quadratic or cubic function (Therrien *et al.*, 2010). The one applied in this study is an RDF constant function recommended for shallow-depth crops (Feddes & Raats, 2004) such as tef crop.

The moisture content dependence term f_2 (θ) relates the transpiration rate to different saturation degrees as given in Equation 9, with the maximum value between the moisture content at field capacity (θ_{fc}) and the oxic limit (θ_{ox}), while decreasing to zero at the wilting point (θ_{wp}) and the anoxic limit (θ_{an}).

The dimensionless fitting parameter C_3 determines the rate of f_2 (θ) change with θ and becomes linear for C_3 equal to 1, as is commonly assumed.

$$f_2(\theta) = \begin{cases} 0, \ for\ 0 \le \theta \le \theta_{wp} \\ f_3 \quad for\ \theta_{wp} \le \theta \le \theta_{fc} \\ 1 \ for\ \theta_{fc} \le \theta \le \theta_{ox} \\ f_4 \ for\ \theta_{ox} \le \theta \le \theta_{an} \\ 0 \ for\ \theta_{an} \le \theta \end{cases} \quad (9)$$

Where:

$$f_3 = 1 - \left[\frac{\theta_{fc} - \theta}{\theta_{fc} - \theta_{wp}}\right]^{C_3} \quad (10)$$

and

$$f_4 = 1 - \left[\frac{\theta_{an} - \theta}{\theta_{an} - \theta_{ox}}\right]^{C_3} \quad (11)$$

The soil water evaporation, E_s, can be simulated by two different models (Therrien *et al.*, 2010). The one used in this study is the one where E_s is assumed to occur along with transpiration and is calculated as follows:

$$E_s = \alpha^*\left(E_p - E_{CAN}\right)[1 - f_1(LAI)]EDF \qquad (12)$$

Where: α^* is the wetness factor that is used to describe the moisture availability for the subsurface domain (Allen *et al*., 1998). EDF is the evaporation distribution function describing the reduction of the energy penetration with depth.

In Situ Water and Soil Conservation Practices

The effects of two *in situ* WSC practices, *terwah*+ (TER+) and *derdero*+ (DER+) on rainwater partitioning were simulated and compared with the conventional tillage (CT) practice in the study area. These two practices are the recent modifications of *terwah* and *derdero* traditional *in situ* WSC practices that have widely been used in Tigray to control soil erosion. The modifications were introduced to improve their efficiency not only in reducing runoff but also in soil quality improvement, soil fertility as well as increasing crop yields (Nyssen *et al*., 2011; Tesfay Araya *et al*., 2011). In TER+ practice, contour furrows of about 0·2 m wide and 0·1 m deep are created at 1·5 m intervals between permanent broad beds, whereas in DER+, permanent raised beds of 0·6 m width with furrows of about 0·2 m wide and 0·1 m deep are created to prevent water logging and collect excess water that would otherwise runoff (Figure 2, top). The plus sign (+) in both practices represents retaining at least 30% of crop residue after a cropping season, minimum tillage of the beds and crop rotations to comply with the principles of conservation agriculture. In CT (control), no contour furrows are made, and at least three tillage practices are carried out with complete removal of crop residue. Full descriptions of these *in situ* WSC practices are given by Nyssen *et al*. (2011).

Model setup, initial and boundary conditions

Three grids (Figure 2, bottom) representing CT, TER+ and DER+ *in situ* WSC practices were constructed using grid builder programme, on the basis of the plot measurements (5 × 19 m) and slope (3%). Grid builder is a pre-processor software with inbuilt graphical interface and capabilities to generate two-dimensional finite element grids. Full description of grid builder can be found in the manual by McLaren (2007). The choice of grid builder in this study relates to its compatibility with the HGS model software. Prior to grid generation, text files of elevation data and grid dimensions (x = 0·1 m and y = 0·1 m) were prepared and exported to grid builder. For each plot, two layers (base and top) were generated using edit node property options and were saved as node property files (*nprop). The top layers of TER+ and DER+ were further transformed to include furrows of 0·2 m wide and 0·1 m deep at regular intervals of 1·5 and 0·6 m for TER+ and DER+, respectively. Finer grids (0·05 × 0·05 m) were used at the furrows. All the grid files were copied to the respective grid builder working folders of the three practices in HGS. The two-dimensional grids were extended to a depth of 1 m to generate the three-dimensional grids (Figure 2, bottom). Through the grid builder, evapotranspiration was also introduced into the HGS model by assigning some parts of the surface layer as evaporating elements and saving such a file with extension (*eprop).

The initial conditions specified included the initial head and initial degree of soil saturation. With the assumption that, the soil is very dry prior to the start of the rainy season, the water saturation degree of 0·2 corresponding to initial head of −10,000 cm was obtained from the water retention curve and was taken as initial soil condition. Simulations were started on 1 January (5 months before the onset of the rainy season) to ensure that the initial conditions imposed very little influence on the outcome of the simulations.

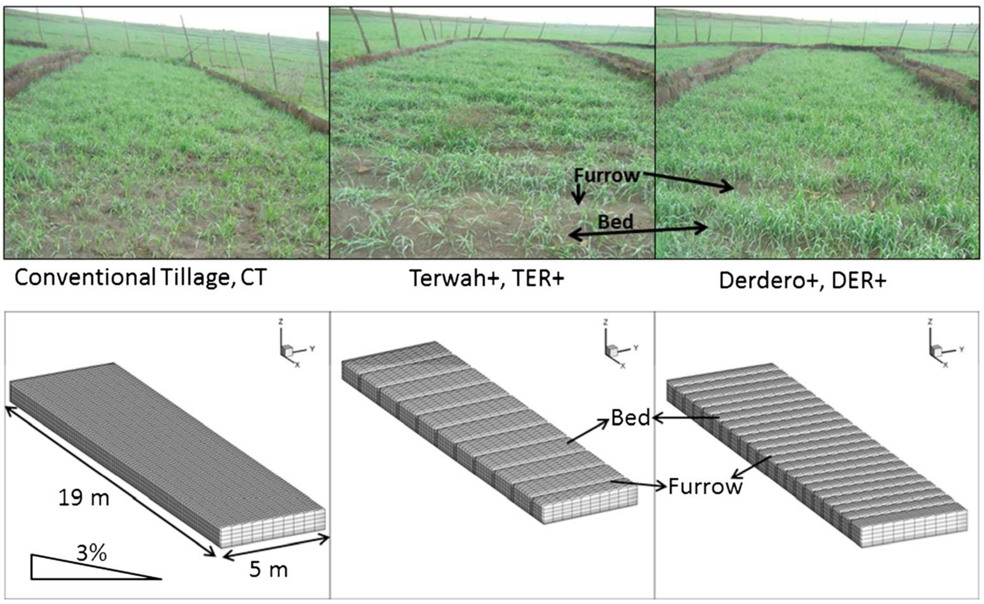

Figure 2. Top: field view of conventional tillage, terwah+ and derdero+. Bottom: model setup of conventional tillage, terwah+ and derdero+ tillage practices. This figure is available in colour online at wileyonlinelibrary.com/journal/ldr.

Rainfall and evapotranspiration expressed as flux ($cm\,min^{-1}$) were imposed as boundary conditions at the surface layer, whereas free drainage (also a boundary condition) was imposed at the bottom faces and the lateral domains of the grid, allowing soil water to freely leave the soil system. As in the field, runoff was collected at the bottom of the plots.

Determination of HydroGeoSphere Model Input Parameters

HydroGeoSphere requires an input of van Genuchten parameters (residual moisture content θ_r, saturated moisture content θ_s, scaling parameter α, pore connectivity factor, and shape parameters n and m) as well as saturated hydraulic conductivity, K_{sat}, to describe subsurface flow. Manning coefficients (friction factors in both x and y directions) are required for simulating surface flow, whereas coupling length is needed to describe surface–subsurface exchange flow. Crop parameters are also required for simulation of the evapotranspiration process.

Initial estimates of the van Genuchten parameters were obtained from soil water retention curves (SWRC) that were established from six undisturbed soil samples taken from each plot using standard sharpened steel 100 cm^3 Kopecky rings at different depths of 0–0·1 m, 0·1–0·2 m and 0·3–0·4 m. Full description of the SWRC determination is given by Tesfay Araya (2012). Field saturated hydraulic conductivity (K_{fs}) was obtained by Tesfay Araya (2012) as described by Reynolds *et al.* (2002).

Briefly, this parameter was measured using single ring with constant head method described in Reynolds *et al.* (2002). A total of six measurements per plot were carried out at the interval of 2 weeks, each time taking two measurements per plot. The metal ring of diameter 0·22 m and height of 0·25 m was carefully driven into the soil to a depth of 0·03 m. The ring was carefully filled with water up to the required constant head, H of 0·05 m, and this head was kept constant by using the Mariotte system of a Guelph permeameter® (Soilmoisture Equipment, Santa Barbara, CA, USA) (Verbist *et al*., 2010).

Readings of water height in the reservoir (cm) were taken every minute from the outer cylinder Guelph for a period of at least 1 h. The average value of the last 10 min was taken as the final infiltration rate, and q was calculated as follows:

$$q = \frac{h_2 - h_1}{t_2 - t_1} * \frac{A_{\text{Guelph}}}{A_{\text{ring}}} \tag{13}$$

Where: h is water height (cm) in the reservoir, t is time, subscripts 1 and 2 indicate two successive readings, $A_{G\text{uelph}}$ is the inner surface of the reservoir (m^2) and A_{ring} is the surface of the ring (m^2).

Field saturated hydraulic conductivity, K_{fs} was then calculated from infiltration rate measurements using Reynolds & Elrick (1990) equation 14 relating ponded infiltration and K_{fs}.

$$K_{fs} = \frac{q_s}{\frac{H}{C_1 d + C_2 a} + \frac{1}{\alpha^* \, (C_1 d + C_2 a)} + 1} \tag{14}$$

Where: q_s is the quasi-steady infiltration rate [LT^{-1}], a is the ring radius [L], H is the steady-state depth of the ponded water in the ring [L], d is the depth of ring insertion into the soil [L], C_1 and C_2 are dimensionless empirical constants equal to 0·316π and 0·184π respectively for $d \geq 0{\cdot}03$ m and $H \geq 0{\cdot}05$ m, and α^* (value of 0·12 was used) is the macroscopic capillary length [L^{-1}].

Manning coefficients for cultivated field were taken from Manning's n reference tables (Manning's n Values). Sensitivity analysis as described by Verbist *et al.* (2012) showed that these coefficients were less sensitive to both surface runoff and soil moisture content. All three practices therefore received the same value of 0·035 [$L^{-1/3}T$].

The coupling length is based on the virtual surface–subsurface interface and cannot be directly measured. Verbist *et al.* (2012) in the semi-arid environment of Chile demonstrated that coupling length is the most sensitive parameter in simulating both surface runoff and soil moisture. In this study, coupling length was determined during model parameter optimization. The initial value was set at 0·01 m. All input parameters to describe surface–subsurface flow are summarized in Table I.

Daily potential evapotranspiration (PET) was calculated from measured daily E_{pan} following the method given by Allen *et al.* (1998). The HGS model uses PET to calculate actual transpiration that also depends on the crop. In this study, teff (*Eragrostis tef*) and wheat (*Triticum spp.*) were crops grown in cropping seasons of 2009 and 2010 and were considered during model calibration and verification. Transpiration fitting parameters and evaporation saturation limits required by the model for simulation of evapotranspiration were not available for teff crop. Because teff crop is similar to grass, this study utilized some parameters described for grass and found in the work of Therrien *et al.* (2010). Field capacity (θ_{fc}) and permanent wilting point (θ_{wp}) for both wheat and teff were obtained from SWRC described by Tesfay Araya (2012) by curve fitting. Maximum rooting depth of teff was reported to be 0·5 (Vanuytrecht, 2007) and 0·9 m for wheat (FAO, 2009). Table II gives all parameters and their values used for simulation of evapotranspiration and interception for both teff and wheat.

Model Parameter Optimization and Calibration

Calibration and validation of the model were performed to match the model simulations to the measured runoff and soil moisture. Field measured runoff and soil moisture data for the 2009 and 2010 growing seasons (described by Tesfay Araya *et al*., 2012) were used for model calibration and verification. Briefly, trenches of about 4·5 m long, 1·5 m wide and 1 m deep were dug at the lower end of each plot and lined with 0·5-mm thick plastic sheets for runoff and sediment collection. Surface runoff inflow and outflow from the experimental plots was avoided by placing iron sheets at the surrounding border of each plot except to one side where the deep collector trenches were located and by separating the plots with 0·5-m wide ditches (Tesfay Araya, 2012). The average water depth from three different positions in each trench was taken every morning (8:00) after the rainfall event that generated runoff. Because of the swelling and shrinking

Table I. Initial values of all the parameters required for simulation of surface–subsurface water flow, standard deviation (of the measured parameters), and the estimated values and confidence intervals from parameter estimation (only for parameters that were calibrated)

Treatment		Parameter						
		K_{fs}	θ_r	θ_s	α	n	Coupling length	x- and y-friction factor
Derdero+	Initial value	6·667	0·000	0·571	0·015	1·671	0·010	0·035
	SD	5·000	–	0·018	0·002	0·079	–	–
	Estimated	6·433	–	0·482	–	–	0·680	–
				95% Confidence interval				
	Lower limit	2·630	–	0·305	–	–	0·110	–
	Upper limit	7·215	–	0·600	–	–	1·350	–
Terwah+	Initial value	6·667	0·000	0·550	0·016	1·654	0·010	0·035
	SD	10·000	–	0·013	0·003	0·124	–	–
	Estimated	6·917	–	0·412	–	–	0·700	–
				95% Confidence interval				
	Lower limit	2·530	–	0·205	–	–	0·050	–
	Upper limit	11·715	–	0·610	–	–	1·250	–
Conventional tillage	Initial value	5·000	0·000	0·556	0·015	1·674	0·010	0·035
	SD	3·333	–	0·016	0·014	0·402	–	–
	Estimated	6·467	–	0·401	–	–	0·530	–
				95% Confidence interval				
	Lower limit	2·744	–	0·178	–	–	–0·250	–
	Upper limit	10·020	–	0·570	–	–	1·720	–
	Units	$\times 10^{-7}$ m s^{-1}	m^3 m^{-3}	m^3 m^{-3}	m^{-1}	–	m	s m$^{-1/3}$

van Genuchten parameters (θ_r, θ_s, α and n) were obtained by curve fitting to water retention data reported by Tesfay Araya (2012) from the same field plots as in this study; initial values for K_{fs} were taken from data reported by Carpentier (2011); x- and y-friction values were taken from literature (Manning n tables) for cultivated field.
K_{fs} is the field saturated hydraulic conductivity, θ_r is the residual moisture content, θ_s is the saturated moisture content, α is the scaling parameter and n is the shape parameter. SD is standard deviation of the mean ($n = 6$).

nature of the Vertisols, the volume of the trenches would vary with time. Therefore, trenches were calibrated annually in the middle of the growing season on the basis of known amounts of water and water depth at three sample locations in each trench following procedures by Gebreegziabher *et al*. (2009) and Oicha *et al*. (2010).

Table II. Input values into the model for simulation of evapotranspiration

Parameter	Value for teff	Value for wheat	Unit
Transpiration fitting parameters			
C1	0·50	0·50	–
C2	0·00	0·00	–
C3	1·00	1·00	–
Transpiration limiting saturations			
Wilting point	0·41	0·45	% Saturation
Field capacity	0·61	0·70	% Saturation
Oxic limit	0·75	0·75	% Saturation
Anoxic limit	0·90	0·90	% Saturation
Evaporation limiting saturations			
Minimum	0·22	0·22	% Saturation
Maximum	0·90	0·90	% Saturation
Leaf area index	1·00	1·00	–
Root zone depth	0·50	0·90	m
Evaporation depth	0·50	0·90	m
Canopy storage parameter	0·04	0·04	m
Initial interception storage	0·04	0·04	m

Wilting point and field capacity values for teff and wheat were obtained from soil water retention curve described by Tesfay Araya (2012). Rooting depth of teff and wheat was obtained from the work of Vanuytrecht (2007) and FAO (2009), respectively. All the other remaining parameters were default values provided for grass and described by Therrien *et al*. (2010).

The soil moisture content was measured using the gravimetric method. A total of six soil samples per soil depth per treatment were taken at 0·2 m intervals up to a depth of 1 m using an auger. Fresh weights of these samples were taken in the field before they were transported to the laboratory. Samples were oven-dried at 105 °C for 24 h, and their dry weights were measured. Gravimetric soil moisture content (w) was calculated using Equation 15:

$$w = \frac{Mw}{Ms} \tag{15}$$

Where: Mw and Ms are the mass of water and mass of dry soil, respectively.

Gravimetric moisture content was converted to volumetric moisture content (θ) using the bulk density obtained following procedures described as follows:

The soil shrinkage characteristic curve describing the volume change of Vertisols with change in moisture content was determined using the equation suggested by Cornelis *et al.* (2006):

$$e(\vartheta) = e_o + \gamma\left[exp\left(\frac{-\varepsilon}{\vartheta^c}\right)\right] \tag{16}$$

Where: ϑ is the moisture ratio, e_o is the void ratio at oven-dryness and γ, $-\varepsilon$ and c are fitting parameters.

Moisture ratio, ϑ ($m^3 m^{-3}$), was calculated from the following equation:

$$\vartheta = \frac{\rho_s}{\rho_w} . w \tag{17}$$

Where: ρ_s is particle density ($mg\, m^{-3}$) and ρ_w is density of water, taken at $1\, mg\, m^{-3}$.

Void ratio, e ($m^3 m^{-3}$), is calculated as follows:

$$e = \frac{\rho_s}{\rho_b} . -1 \tag{18}$$

Finally, the bulk density, ρ_b, was obtained by combining Equations 16 –17, and θ was derived from Equation 19:

$$\theta = \frac{\rho_b}{\rho_w} . w \tag{19}$$

Volumetric moisture content was concurrently recorded until 1 m depth using a Trime® water sensor (IMKO Micromodultechnik GmbH, Ettlingen, Germany). However, the data appeared to be unreliable in the swelling and shrinking clay soil under study (Tesfay Araya *et al.*, 2014b) and were therefore not further used in this study.

Lack of detailed measurements of rainfall intensity data for the complete period under study presented a major challenge during the calibration and validation of the model. An average rain intensity value was used in this case and incorporated into the measured daily rainfall.

Parameter estimation software (Doherty, 2010) was used for automatic parameter optimization. The Levenberg–Marquardt minimization procedure was used to determine a minimum value of the objective function. For this study, an objective function (Φ) (Equation 20) was defined to minimize the difference between observed and simulated runoff and soil moisture contents:

$$\Phi[\theta(t), R(t)] = \sum_{i=1}^{n_\theta} u_i[\theta_o(t_i) - \theta_s(t_i, \beta)]^2 + \sum_{i=1}^{n_R} v_i[R_o(t_i) - R_s(t_i, \beta)]^2 \tag{20}$$

Where: θ and R represent soil moisture content and runoff, respectively, and t is the measurement time. β represents the optimized parameter set, u and v are weighing factors for individual measurements and measurement types determined using the method described by Hopmans *et al.* (2002), n_θ and n_R are the number of observations for the soil moisture and runoff measurements respectively and the subscripts o and s respectively refer to observed and simulated values.

Using both runoff and soil moisture contents in the optimization process enables an evaluation of the model capacity to optimize both surface and subsurface processes simultaneously using appropriate weighting (Verbist *et al.*, 2012). Parameter estimation makes several model runs by changing free parameters until the closest values between measured and simulated are realized.

Full sensitivity analysis to determine the adjustable model parameters during optimization was not carried out. However, an earlier similar study in a semi-arid environment by Verbist *et al.* (2012), in which variance-based global sensitivity analysis using Jansens' estimator (Jansens, 1999) was applied, showed that coupling length and K_{fs} were the most sensitive parameters to both surface runoff and soil moisture simulation. Parameters α, n and θ_s were also shown to be sensitive with the latter parameter playing an important role in subsurface water redistribution (Verbist *et al.*, 2012). In this study, we kept α and n to their initial values and only calibrated coupling length, K_{fs} and θ_s. Pore connectivity factor (l), θ_r and x- and y-friction factors were found to be insensitive to both surface and subsurface processes (Verbist *et al.*, 2012). A fixed value of 0·5 (Mualem, 1976) was therefore used for l across all the three practices. Residual moisture content (θ_r), x- and y-friction factors were also fixed to their initial values (Table I).

Residual mean squared error (RMSE; Equation 21), Pearson correlation coefficient (ρ; Equation 22) and Nash–Sutcliffe model efficiency (E; Equation 23) were computed to evaluate the goodness of fit between measured and HGS simulated runoff and soil moisture contents across all the three tillage practices:

$$RMSE = \sqrt{\frac{\sum_{i=n}^{N}[X_i - O_i]^2}{n}} \tag{21}$$

$$\rho = \frac{\sum(X_i - \overline{X}_i)\ (O_i - \overline{O}_i)}{\sqrt{\sum(X_i - \overline{X}_i)^2 (O_i - \overline{O}_i)^2}} \tag{22}$$

$$E = \sqrt{\frac{\sum_{i=n}^{N}[X_i - O_i]^2}{\sum_{i=n}^{N}[X_i - \overline{X}_i]^2}} \tag{23}$$

Where: n is the number of measurements, x_i and o_i are the measured and predicted values respectively, and $\overline{X}_i$ and $\overline{O}_i$ are the average of the measured and predicted values, respectively.

Soil Water Balance and Relative Crop Yield as Influenced by In Situ WSC Practices

Rainwater partitioning as influenced by TER+ and DER+ practices was calculated for dry and wet years. Tesfay Araya (2012) has analysed 31 years of rainfall data using the RAINBOW software (Raes *et al.*, 2006). A year was qualified dry, wet or normal on the basis of the probability of non-exceedance (PONE) values. According to their results, the year 2005 falls under a dry year (PONE = 18%); 2006 and 2010 were wetter than normal years (PONE = 81% and 78%, respectively). The year 2009 was drier than normal with PONE of 28%.

Only wheat was considered for water balance, and relative yields calculations as parameters for teff (e.g. crop coefficients, Kc, and crop yield factor, Ky) could not be obtained. The water balance components included rainfall (P), runoff (RO), actual transpiration (T_p), surface evaporation (E_p), subsurface evaporation (E_s) and deep drainage (D). Except for P, which was obtained from measurements, all the other components were extracted from the model overland, hydrographs and water balance output files. The overall change in water storage (ΔS) within the rootzone for each practice was obtained by solving the soil water balance equation 24:

$$\Delta S = P - RO - T_p - E_p - E_s - D \tag{24}$$

Relative yield (*Ya*/*Ym*) was calculated on the basis of the approach by Doorenbos & Kassam (1979):

$$1 - Ya/Ym = Ky*(1 - AET/ETc) \tag{25}$$

Where: *Ya* is actual crop yield on the basis of the field conditions, *Ym* is the maximum crop yield under no water stress conditions and *Ky* is the crop yield factor describing the response of crop yield to water stress [$Ky = 1$ was used in this study. This value was given in data description-FAST5 (http://www.fao.org/giews/english/shortnews/DataDescription Fast5.pdf) for wheat in Ethiopia].

The *AET* is the actual crop evapotranspiration during the growing season, and it was obtained as follows:

$$AET = T_p + E_p + E_s \tag{26}$$

Where: T_p (actual transpiration), E_s (subsurface evaporation) and E_p (surface evaporation) are all outputs from HGS model.

The *ETc* is the maximum crop evapotranspiration under standard conditions calculated as follows:

$$ETc = Kc*PET \tag{27}$$

The growing season of wheat was from June to September, and four different *Kc* values (corresponding to initial, development, mid and late season growth stages) for spring wheat were obtained from FAO website (http://www.fao.org/nr/water/cropinfo_wheat.html). Each of these values was multiplied by PET for that month to obtain the *ETc* for the respective month. The sum of *ETc* from 4 months was the value used in Equation 25 to calculate *Ya*/*Ym*.

RESULTS

Model Performance

Results of the HGS model performance as reflected by the RMSE, ρ and E values for 2009 (model calibration) and 2010 (model verification) are summarized in Table III. Generally, low values of RMSE and high values of ρ and E depict good agreement between measured and HGS simulated runoff and moisture contents. Additionally, Figure 3 shows good agreement between simulated and observed runoff values for CT, TER+ and DER+ tillage practices following rainfall events from 20 July until 2 September 2010. In general, HGS simulated total runoff values were close to measured total runoff values for all treatments. The model, however, performed poorer in simulating runoff under CT (Table III). Figure 4 shows the results of simulated soil moisture content as compared with measured moisture content. Generally, the model simulated results were close to the measured moisture content across all the tillage practices.

Table III. Residual mean squared error (RMSE), Pearson correlation coefficient (ρ) and Nash–Sutcliffe model efficiency (E) for simulated runoff and moisture content for DER+, TER+ and conventional tillage (CT) practices

Year		DER+	TER+	CT
2009	Runoff			
	RMSE (mm)	0·95	2·09	2·77
	ρ (%)	88·0	89·0	87·0
	E	0·58	0·61	0·52
	Soil moisture content			
	RMSE (m^3m^{-3})	0·03	0·03	0·02
	ρ (%)	84·0	86·6	88·0
	E	0·60	0·75	0·74
2010	Runoff			
	RMSE (mm)	1·15	2·02	3·09
	ρ (%)	92·0	92·0	81·0
	E	0·70	0·79	0·23
	Soil moisture content			
	RMSE (m^3m^{-3})	0·03	0·03	0·03
	ρ (%)	93·0	94·0	75·0
	E	0·83	0·80	0·16

Note that 2009 runoff and moisture data were used of calibration, whereas 2010 runoff and moisture data were used for model verification.

Effect of In Situ Soil Water Conservation Practices

Total simulated water balance components for dry and wet years for each *in situ* WSC practice under wheat are summarized in Table IV. These results indicate that DER+ practice results in low runoff generation followed by TER+, whereas CT is associated with higher runoff generation across all the years. For example, about 8% of the rainfall is lost as runoff (*RO*) under DER+ and TER+ compared with 31% under CT practice in a wet year of 2010 (Table IV).

Actual evapotranspiration, *AET* (i.e., $T_p + E_s + E_p$), was generally higher in DER+ and TER+ compared with CT. In a wet year of 2010, for example, DER+ had the highest *AET* (131 mm) followed by TER+ (108 mm) and the lowest under CT (46 mm) (Table V). Drainage was the main unproductive water loss only in wet years especially for DER+ and TER+ tillage practices (Table IV). Subsurface evaporation, E_s, accounted for 16%, 14% and 6% of the total rainfall in 2010 lost under DER+, TER+ and CT, respectively. Model results generally showed logical trends (across all three practices) in rainwater partitioning, with wet years showing higher water balance components (*RO*, T_s, E_s, E_p), whereas the lowest values of these components are found in a dry year.

Soil moisture distribution under wheat in 2010 both at the soil surface and subsurface as influenced by DER+ and TER+ tillage practices can be clearly visualized in Figure 5. It can be seen that DER+ has more soil moisture distributed throughout

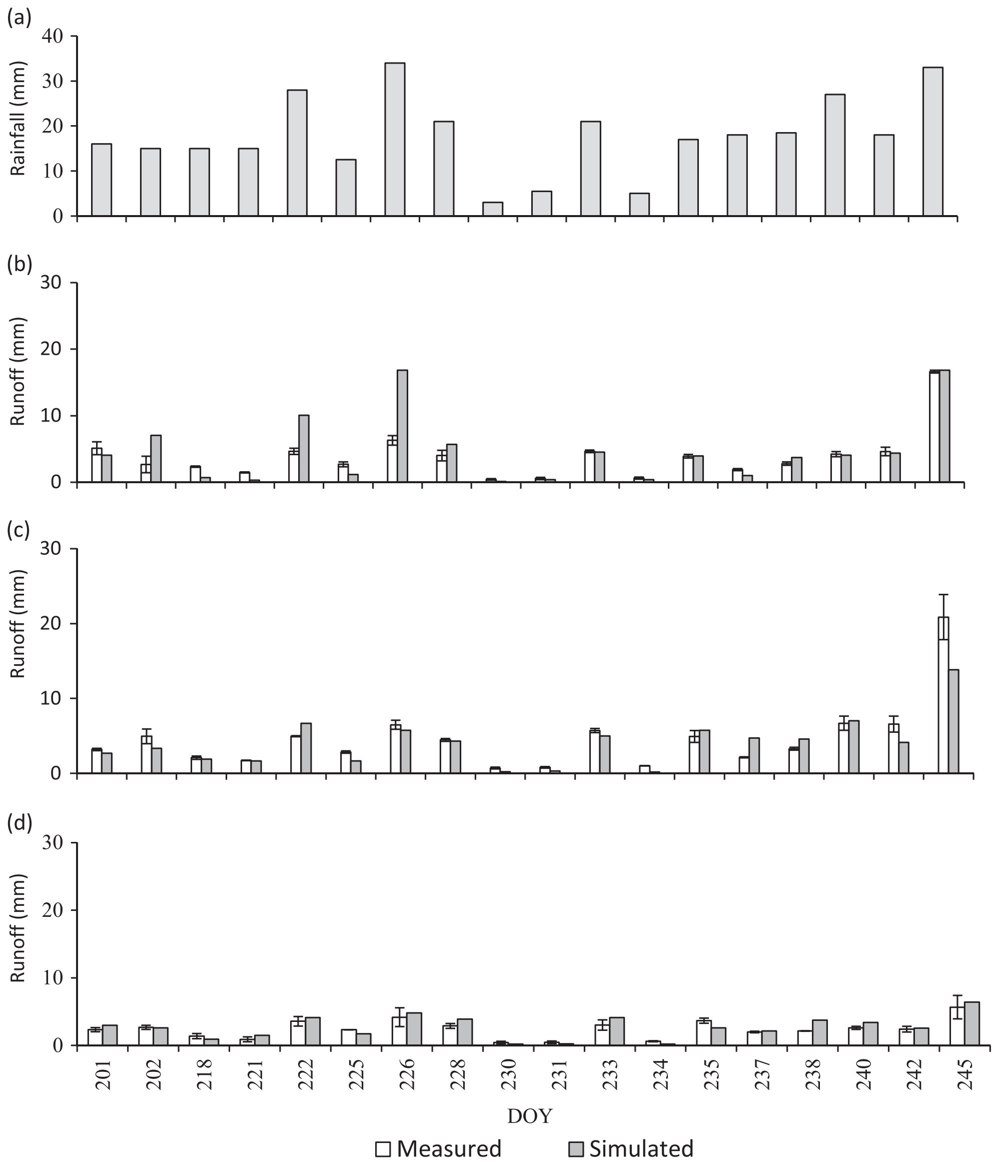

Figure 3. Precipitation (a) and comparison between HGS simulated runoff and measured runoff for CT (b), TER+ (c) and DER+ (d). The error bars show the standard error of the mean of measured values. Day of the year (DOY) 201 and 245 correspond to 20 July 2010 and 2 September 2010, respectively.

the root zone because of its closely spaced furrows. TER+ is as well more effective than CT as the furrows collect water and slowly distribute it into the lower soil depth.

Relative yields (*Ya*/*Ym*) of wheat crop as influenced by *in situ* WSC practices are shown in Table V. As expected, simulated *Ya*/*Ym* values were higher in wet years compared with that of dry years. In general, relative yields were highest under DER+ followed by TER+ and lowest under CT.

DISCUSSION

Potential of HydroGeoSphere to Simulate the Effects of In Situ WSC

The measured runoff and soil moisture content across all the three tillage practices were generally reproduced by the model. However, discrepancies between simulated and measured values were observed. These differences could be explained by the fact that rainfall intensity used was an average value. Scaling parameter α and shape parameter n whose values were fixed to the initial measured values could also have had influence on the runoff output especially in the beginning of the rainy season (Verbist *et al*., 2012). The model simulated results however followed the logical trends as the measured runoff increased with higher rainfall producing higher surface runoff. These results have demonstrated that HGS model has a great potential to simulate the effects of *in situ* WSC practices.

Effect of TER+ and DER+ In Situ Soil Water Conservation Practices

Simulated results show that DER+ and TER+ significantly reduced rain water loss through runoff compared with CT. Runoff coefficients for DER+ and TER+ are lower than (except for TER+ in 2006) the values reported in the

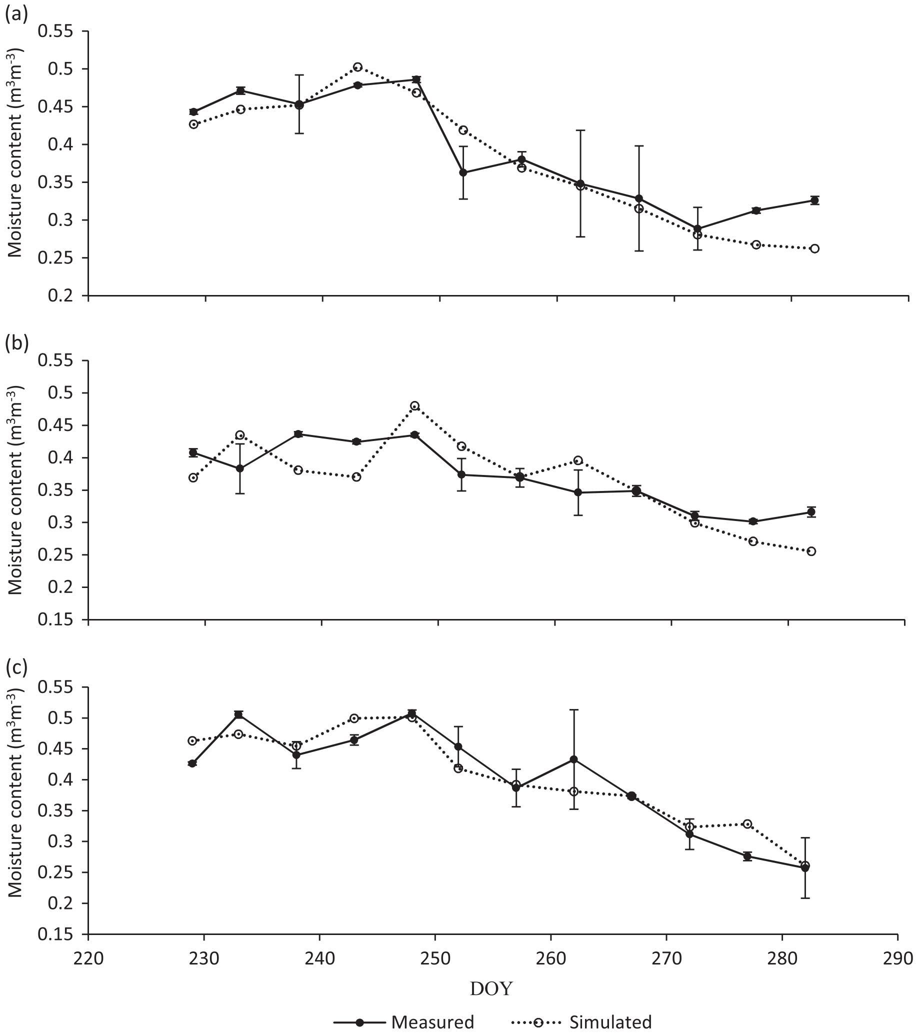

Figure 4. Comparison between HGS simulated and measured moisture content at 0·15 m depth for CT (a), TER+ (b) and DER+ (c). The error bars show the standard error of the mean of measured values. The period of simulation was between 17 August 2010 [day of the year (DOY) = 229] and 9 October 2010 (DOY = 282).

findings from a synergy of results from sub-Saharan Africa research (Falkenmark & Rockström, 2008) in which between 10% and 25% of rainfall is reported to be lost as *RO* under controlled experiments. The significant reduction of runoff under DER+ and TER+ was ascribed to the combined effect of minimum tillage, stubble crop residue, and furrow and bed structures. For this study, this effect can only be explained by the presence of furrow and bed structures.

Table IV. Soil water balance components for DER+, TER+ and conventional tillage (CT) practices calculated for dry and wet years

Year	Condition	Treatment	*P*	*RO*	*T*	E_s mm	*Ep*	*D*	ΔS
2005	Dry	DER+	287	8	17	17	2	0	243
		TER+	287	8	38	25	0	0	217
		CT	287	36	8	12	0	0	230
2006	Wet	DER+	541	50	22	57	9	237	166
		TER+	541	67	20	44	3	184	223
		CT	541	160	10	38	0	0	333
2009	Dry	DER+	355	20	27	40	0	0	269
		TER+	355	46	50	23	0	0	237
		CT	355	95	12	18	0	0	230
2010	Wet	DER+	500	41	45	81	5	64	264
		TER+	500	38	37	70	1	131	223
		CT	500	155	12	34	0	1	298

All calculations were based on the 4 months (June to September) of the growing season. *P* is rainfall, *RO* is runoff, T_p is actual transpiration, E_s is soil evaporation, E_p is surface evaporation, *D* is deep drainage and ΔS is change in water storage.

Table V. Relative yields of wheat calculated for dry and wet years under practices DER+, TER+ and conventional tillage (CT)

Year	Treatment	*AET* (mm)	*ETc* (mm)	*Ya*/*Ym*	Observed yields (t ha^{-1})*
2005	DER+	35	250	0·14	2·30
	TER+	63	250	0·25	1·97
	CT	20	250	0·08	1·53
2006	DER+	88	271	0·32	
	TER+	67	271	0·25	
	CT	48	271	0·18	
2009	DER+	67	243	0·28	2·60
	TER+	73	243	0·30	1·90
	CT	30	243	0·12	1·60
2010	DER+	131	216	0·61	
	TER+	108	216	0·50	
	CT	46	216	0·21	

AET is actual evapotranspiration, and *ETc* is crop evapotranspiration.
*Observed grain yields reported by Tesfay Araya (2012).

According to Nyssen *et al.* (2011) and Tesfay Araya *et al.* (2011), furrow and bed structures reduce the water velocity and collect the excess water that will slowly infiltrate into the soil and become available for plant use. Lanckriet *et al.* (2012) demonstrated that furrows increase ponding time and consequently increase the amount of water infiltrating into the soil while reducing surface runoff. Verbist *et al.* (2012) used a modelling approach and demonstrated that trenches in a wet year significantly reduced surface runoff and effectively harvested up to 64% of the potential runoff. They attributed this to the capacity of trenches to accumulate water and enhance its storage in the soil profile.

The effects of *in situ* WSC on soil water balance components especially drainage were pronounced in wet years compared with dry years. The possible explanation for higher drainage under DER+ and TER+ could be attributed to the greater amount of water collected in the furrows that is consequently available to freely infiltrate into the deeper part of the soil profile. In CT practice, however, significant amount of the rain water is lost through runoff (Table IV), and consequently, less water is available for deep drainage. Verbist *et al.* (2012) also reported in a wet year a clear increase in drainage component when trenches are used. They attributed this effect to the increased retention and infiltration of the potential runoff in the trench. Similar explanations hold for the E_s that was among the main water balance and increased from dry year to wet year.

Although DER+ and TER+ practices have demonstrated a significant reduction in runoff losses and increase in *AET* compared with CT, more of the water in a wet year is lost through deep drainage. Indeed, our 2006 simulations in which around 43% and 37% of the rainfall was lost through deep drainage under DER+ and TER+ respectively were even outside in the range of 10–30% reported by (Rockström & Falkenmark, 2000; Falkenmark & Rockström, 2008) from on-farm research on water partitioning in savannah dry land cropping systems in sub-Saharan Africa. There is therefore need for further improvement in the techniques (DER+ and TER+) in order to improve the amount of water that goes to transpiration. Reducing deep drainage losses can be achieved

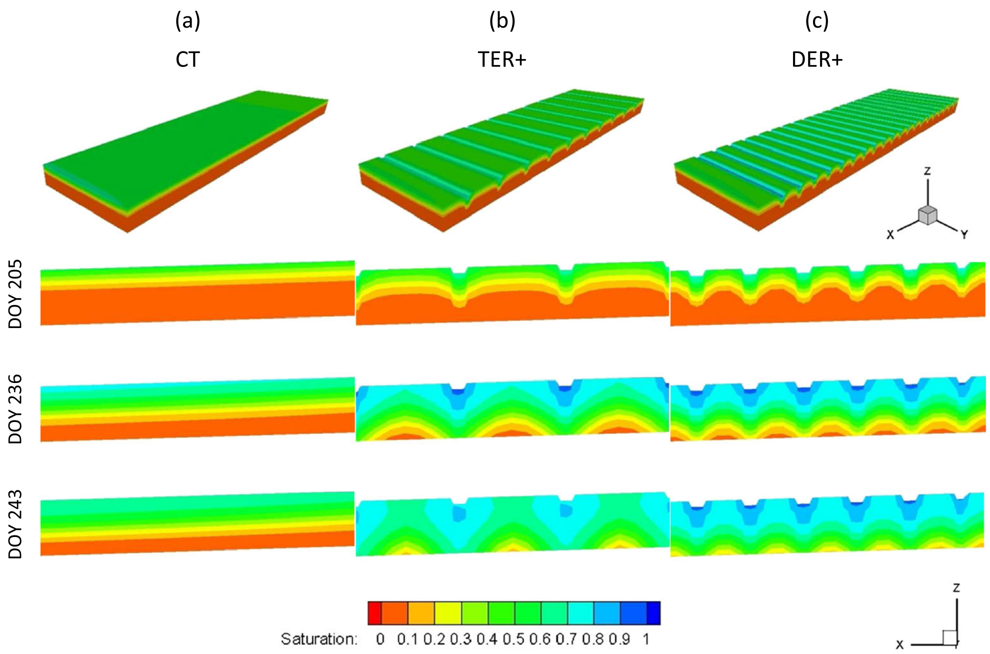

Figure 5. Upper panel: three-dimensional representation of simulated water content expressed as saturation degree as influenced by CT (a), TER+ (b) and DER + (c). Lower panel: vertical two-dimensional slice of the soil domain at a point, $y = 2{\cdot}5$ m, showing simulated water content expressed as saturation degree at three different dates in 2010: after a rainfall event of 9·5 mm (DOY 205) and after a rainfall event of 21 mm (DOY 236). No rainfall event was recorded on DOY 243, but at total rainfall of 49 mm was received between DOY 237 and DOY 243. Notice higher water content indicated by the saturation degree (blue colour) in DER+ closely followed by TER+. DOY is day of the year from the Julian calendar. This figure is available in colour online at wileyonlinelibrary.com/journal/ldr.

by adding more organic matter to the soil to increase water holding capacity and intercropping annual crops with perennial species such as trees that generally have deeper root systems and are more effective in extracting soil water and reducing drainage. There is however need for research to find tree/crop mixtures that are feasible and at the same time enable to make better use of the available water resources (Wallace, 2000).

Introducing furrows at much closer intervals as in DER+ significantly increases the amount of water that can slowly infiltrate and distribute into the soil. From Figure 5, it can be visualized that furrows accumulate water first and slowly distribute it into the raised beds. This implies that presence of these structures can help to minimize the effects of temporal water logging commonly experienced under Vertisols when rainfall is intense (Nyssen *et al*., 2011).

Relative yields reduced towards dry years indicating higher crop water stress as indicated by lowest values of *AET* in dry year (2005) compared with wet year (Table V). These relative yields however have to be treated with care as a sensitive parameter (*Ky*) for wheat was assumed and not calibrated for study area conditions. Differences in relative yields among the practices reduced in the wet years probably because of less chances of crop water stress at sensitive growth stages in the wet year compared with dry year. Data on the potential yields (*Ym*) of wheat in the study area were not available thus limiting our ability to evaluate the accuracy of the simulated relative yields. However, actual yields obtained from field experiments have been reported by Tesfay Araya (2012) and were used for comparison of trends in relative yields among different practices. Trends in the differences of relative yields among the WSC practices were comparable with trends of measured yields. However, greater differences in simulated relative yields among DER+, TER+ and CT were recorded across all the years compared with the differences in actual yields measured for the three practices (Table V). These differences are due to higher differences in the amounts of simulated *AET* across the three practices with CT recording the lowest values in all the years (Table V). These differences in the yields therefore indicate that *AET* was either overestimated for DER+ and TER+ practices or underestimated for CT practice. In either case and referring to equations 6–12 used for calculating transpiration and evaporation, this would require adjusting the transpiration and evaporation parameter values (Table II), especially those relating transpiration rate to soil moisture saturation (transpiration limiting saturation). However, because of data limitations, no attempt was made to tune these values.

CONCLUSIONS AND RECOMMENDATIONS

HydroGeoSphere (HGS) is a fully coupled surface/subsurface process-based model that was developed to simulate water balances and solute transport on a larger watershed scale. This study applied HGS model to simulate the effects of *in situ* WSC at plot scale. In general, HGS simulated runoff and soil moisture results were close to the measured runoff and moisture content. It can therefore be concluded that HGS is capable of mimicking water flow as affected by *in situ* WSC techniques. The hydrological impact of *in situ* WSC techniques above plot scale is one of the knowledge gaps cited in literature (Falkenmark & Rockström, 2008), and HGS could be used to determine the impact of these techniques on the watershed hydrology.

The HGS simulated results indicate that DER+ *in situ* WSC practice is effective in reducing surface runoff by up to 68% compared with CT and significantly increases soil moisture content. It was observed that the furrows have the capability to collect water and slowly redistribute it to the raised beds. These practices can therefore be used as a strategy to minimize the impacts of temporal water logging that is commonly experienced under the Vertisol soils. Furthermore, this study demonstrated that productive water loss through transpiration was higher under DER+ and TER+ resulting into a higher relative crop yield compared with CT practice. Most importantly, the model was able to split evapotranspiration components into transpiration, soil evaporation as well as surface evaporation. All these water balance components are important for designing of water soil conservation practices.

ACKNOWLEDGEMENTS

This research was funded by the Institutional University Cooperation (IUC) Project in Mekelle University through the Flemish Interuniversity Council (VLIR, Belgium). We are grateful to all the staff of Mekelle University Institutional University Cooperation programme office as well as to the farmers and data collectors for daily activities on the research plot. Emmanuel Opolot benefited from VLIR-UOS scholarship during his Masters studies and from the Belgian Science Policy Office (project : BELSPO/IUAP p7/24) at the time of completion and submission of this article.

REFERENCES

Allen RG, Pereira LS, Raes D, Smith M. 1998. Crop evapotranspiration: guidelines for computing crop requirements. Irrigation and Drainage Paper No. 56 FAO, Rome, 740 Italy.

Boers TM. 1994. Rainwater Harvesting in Arid and Semi-Arid Zones. Publication 55, International Institute for Land Reclamation and Improvement, Wageningen, The Netherlands.

Carpentier L. 2011. The effect of conservation agriculture on the soil quality of a Vertisol and the water productivity of tef (*Eragrostis tef (Zucc*.) Trotter) in Tigray, Ethiopia. Master Thesis, Ghent University; 77.

Cornelis WM, Corluy J, Medina H, Díaz J, Hartmann R, Van Meirvenne M, Ruiz ME. 2006. Measuring and modelling the soil shrinkage characteristic curve. *Geoderma* **137**(1–2): 179–191. DOI:10.1016/j.geoderma.2006.08.022.

Doherty J. 2010. PEST, model-independent parameter estimation user manual: 5th edition 770 Watermark Numerical Computing, Oxley, Australia.

Doorenbos J, Kassam AH. 1979. Yield response to water. FAO Irrigation and Drainage paper No.33.

Falkenmark M, Rockström J. 2008. Building resilience to drought in desertification-prone savannas in sub-Saharan Africa: the water perspective. *Natural Resources Forum* **32**: 93–102.

FAO. 2002. Crops and drops. Making the best use of water for agriculture. Rome, Italy.

FAO. 2009. Crop water information: wheat. http://www.fao.org/nr/water/cropinfo_wheat.html. Accessed on 30/07/2012.

Feddes RA, Raats PAC. 2004. Parameterizing the soil–water–plant root system. Chapter 4, 47p.

Gebreegziabher T, Nyssen J, Govaerts B, Getnet F, Behailu M, Haile M, Deckers J. 2009. Contour furrows for *in situ* soil and water conservation, Tigray, northern Ethiopia. *Soil and Tillage Research* **103**: 257–264.

Hopmans JW, Šimůnek J, Romano N, Durner W. 2002. Inverse Methods. In *Methods of Soil Analysis. Part 4. Physical Methods*, Dane JH, Topp GC (eds). Soil Science Society of America Book Series No. 5. p. 963–1008.

Jansen MJW. 1999. Analysis of variance designs for model output. *Computer Physics Communications* **117**: 35–43.

Jones JP, Sudicky EA, McLaren RG. 2008. Application of a fully-integrated surface-subsurface flow model at the watershed-scale: a case study. *Water Resources Research* **44**: W03407. DOI:10.1029/2006WR005603.

Kristensen KJ, Jensen SE. 1975. A model for estimating actual evapotranspiration 825 from potential evapotranspiration. *Nordic Hydrology* **6**: 170–188.

Lanckriet S, Araya T, Cornelis WM, Verfaillie E, Poesen J, Govaerts B, Bauer H, Deckers J, Haile M, Nyssen J. 2012. Impact of conservation agriculture on catchment runoff and soil loss under changing climate conditions in May Zeg-zeg (Ethiopia). *Journal of Hydrology* **475**: 336–349.

McLaren RG. 2007. Grid builder: a pre-processor for 2D, triangular element, finite element programs. *Groundwater Simulations Group*, University of Waterloo, CA, 93p.

Makurira H, Savenije HHG, Uhlenbrook S, Rockström J, Senzanje A. 2007. Towards a better understanding of water partitioning processes for improved smallholder rainfed agricultural systems: a case study of Makanya catchment, Tanzania. *Physics and Chemistry of the Earth* **32**: 1082–1089.

Manning's n Values: Accessed on 13/04/2012 on the website: http://www.fsl.orst.edu/geowater/FX3/help/8_Hydraulic_Reference/Mannings_n_Tables.htm.

Mualem Y. 1976. A new model for predicting the hydraulic conductivity of unsaturated 871 porous media. *Water Resources Research* **12**: 513–522.

Nyssen J, Govaerts B, Araya T, Cornelis WM, Bauer H, Haile M, Sayre K, Deckers J. 2011. The use of the marasha ard plough for conservation agriculture in northern Ethiopia. *Agronomy for Sustainable Development* **31**: 287–297.

Oicha T, Cornelis WM, Verplancke H, Nyssen J, Deckers J, Behailu M, Haile M, 2010. Short-term effects of conservation agriculture on Vertisols under tef (*Eragrostis tef* (Zucc.) Trotter) in the northern Ethiopian highlands. *Soil and Tillage Research* **106**: 294–302.

Qin H, Cao G, Kristensen M, Refsgaard JC, Rasmussen MO, He X, Liu J, Zheng C. 2013. Integrated hydrological modeling of the North China Plain and implications for sustainable water management. *Hydrology and Earth System Sciences Discussions* **10**: 3693–3741.

Raes D, Willems P, GBaguidi F. 2006. RAINBOW—a software package for analyzing data and testing the homogeneity of historical data sets. Proceedings of the 4th International Workshop on 'Sustainable management of marginal drylands'. Islamabad, Pakistan, 27-31 January (in press).

Reynolds WD, Elrick DE. 1990. Ponded infiltration from a single ring .1. Analysis of steady flow. *Soil Science Society of America Journal*, **54**(5): 1233–1241.

Reynolds WD, Elrick DE, Youns E, Amoozegar A. 2002. Field methods vadose and saturated zone techniques, SSSA, Madison, WI; 817–858.

Rockström J, Falkenmark M. 2000. Semiarid crop production from a hydrological perspective: gap between potential and actual yields. *Critical Reviews in Plant Sciences* **19**: 319–346.

Sciuto G, Diekkrüger B. 2010. Influence of soil heterogeneity and spatial discretization on catchment water balance modeling. *Vadose Zone Journal* **9**: 955–969.

Soltani A, Hoogenboom G. 2007. Assessing crop management options with crop simulation models based on generated weather data. *Field Crops Research* **103**: 198–207.

Tesfay A, Cornelis WM, Nyssen J, Govaerts B, Getnet F, Bauer H, Amare K, Raes D, Haile M, Deckers J. 2012. Medium-term effects of conservation agriculture based cropping systems for sustainable soil and water management and crop productivity in the Ethiopian highlands. *Field Crops Research* **132**: 53–62.

Tesfay A, Nyssen J, Govaerts B, Bauer H, Deckers J, Cornelis WM. 2014a. Impacts of medium term conservation agriculture-based farming systems on optimizing seasonal rainfall partitioning and productivity on Vertisols in northern Ethiopia. *Submitted to Soil and tillage research*.

Tesfay A, Nyssen J, Govaerts B, Bauer H, Gebrehiwot K, Deckers J, Cornelis W. M. 2014b. Effects of seven years resource-conserving agriculture on soil quality in Vertisol of Ethiopian drylands. *Submitted to Soil Research*.

Tesfay A. 2012. Conservation agriculture-based resource saving technology for land resilience in northern Ethiopia. PhD. Thesis, Ghent University.

Tesfay A, Cornelis WM, Nyssen J, Govaerts B, Bauer H, Gebreegziabher T, Tigist T, Raes D, Sayre KD, Haile M, Deckers J. 2011. Effects of conservation agriculture on runoff, soil loss and crop yield under rainfed conditions in Tigray, northern Ethiopia. *Soil Use and Management* **27**: 404–414.

Therrien R, McLaren RG, Sudicky EA, Panday SM. 2010. A three-dimensional numerical model describing fully-integrated subsurface and surface flow and solute transport. Draft; 467.

Vanuytrecht E. 2007. Crop water productivity of Barley and teff in the highlands of Tigray (northern Ethiopia). PhD Thesis, Katholieke Universititeit Leuven; 144.

Verbist K, Cornelis WM, Gabriels D, Alaerts K, Soto G. 2009. Using an inverse modelling approach to evaluate the water retention in a simple water harvesting technique. *Hydrological Earth Systems Science* **13**: 1979–1992.

Verbist K, Pierreux S, Cornelis WM, McLaren R, Gabriels D. 2012. Parameterizing a coupled surface-subsurface three-dimensional soil hydrological model to evaluate the efficiency of a runoff water harvesting technique. *Vadose Zone Journal*. DOI:10.2136/vzj2011.0141

Verbist K, Torfs S, Cornelis WM, Oyarzun R, Soto G, Gabriels D. 2010. Comparison of single- and double-ring infiltrometer methods on stony soils. *Vadose Zone Journal* **9**, 462–475.

Wallace JS. 2000. Increasing agricultural water use efficiency to meet future food production. *Agriculture, Ecosystems and Environment* **82**: 105–119.

Wigmosta MS, Vail LW, Lettenmaier DP. 1994. A distributed hydrology vegetation model for complex terrain. *Water Resources Research* **30**: 1665–1679. DOI:10.1029/94WR00436.

WRB (World reference base for soil resources). 2006. A framework for international classification, correlation and communication. Technical report, FAO.

